TRACE METALS GEOCHEMISTRY IN THREE SEDIMENT CORES FROM THE SKAGGERAK (NORTH SEA)

door

A. Rajendran

Interne Verslagen
s Instituut voor
k der Zee, Texel

I

TRACE METAL GEOCHEMISTRY IN THREE SEDIMENT CORES FROM THE SKAGERRAK (North Sea)

by A. Rajendran

Chemical Oceanography Division, National Institute of Oceanography, Dona Paula, Goa, India 403004

CONTENTS

1. Introduction

The differences in chemistry between marine sediments formed in anoxic and oxic environments have been well documented. Studies have also been carried out to know the differences in the chemical composition of sediments forming in deep-sea environments, in coastal waters or continental shelves. Factors influencing changes in sediments during burial, particularly on the continental shelves, fjords and semi-enclosed seas are only poorly known (PRICE, 1976), despite the fact that these environments are more significant from a geochemical point of view. The shallow-water marine sediments of continental shelves and also semi-enclosed seas receive much organic matter and terrigenous detritus and are consequently more subjected to chemical and biological attack. In this respect, the observations in sediments of the Skagerrak, a small epeiric shelf sea, could offer some useful information on biogeochemical transformations.

The Skagerrak is a 600-700 m deep marine basin between the North Sea and the Baltic Sea, but it is more closely linked to the North Sea (Fig. 1). 50-70% of the total amount of suspended matter deposited in the North Sea, approximately 12-15 million tons per year, is deposited in the Skagerrak, Kattegat and Norwegian Channel (EISMA, 1981). The bulk of the material in suspension is deposited in the eastern and north-eastern part of the Skagerrak (VAN WEERING, 1982). On the basis of the surface circulation pattern and the distribution of suspended matter in the Skagerrak, MULLER & IRION (1984) and EISMA *et al.* (1984) suggest that the particulate matter and associated pollutants may be transported into the Skagerrak chiefly from the English Channel and the Belgian-Dutch-German and English coastal areas, and secondly from the Baltic. They also suggest that the Skagerrak may be regarded as a sink. Additionally, the Skagerrak receives terrestrial runoff sediments and pollutants along the Swedish and Norwegian coast, though a major portion of the particulate matter is trapped in Norwegian fjords (SKEI, 1981). MULLER & IRION (1984) found a general increase in the heavy metal concentrations in the eastern part of the Skagerrak from older to younger sediment layers since about 1870-1880.

This report presents the vertical profiles of different phases of sediment trace metals, namely

(1) carbonate phase
(2) Mn-oxyhydroxide phase
(3) Fe-oxyhydroxide phase
(4) dilute acid leachable fraction
(5) total content of Mn, Fe, Zn, Cu, Co, Ni and As in three cores.

The distribution of porewater oxygen concentration, nitrate, manganese and iron are also presented. These observations were made with the aim to understand the estimates of the steady-state flux of Mn and Fe at the sediment-water interface and also to compare these results with the behaviour of other transient and heavy metals in the Skagerrak.

2. Materials and methods

Sampling:

Sediment samples were collected in the Skagerrak during a cruise with R.V. "Aurelia" in August 1984. For the present study, three cores were selected: two at the south-western flank of the Norwegian channel and one at the centre of the Skagerrak (Fig. 2).

Undisturbed sediment samples were collected with a box corer (600 cm^2 surface area). This corer usually collects a core length of 30-50 cm. Sediment samples for trace metal analysis were collected with a 5.5 cm diameter Plexiglass corer from the central part of the box-core sample. Immediately after retrieval, the box-cored sediment was sampled with the Plexiglass sub-corers and transferred to a N_2-filled glove box. The subcores were then sliced into 0.5 cm sections to a depth of 2.0 cm, 1.0 cm sections down to 4.0 cm and 2.0 cm sections further in downcore. Pore-water samples from the sediment samples were collected with Teflon squeezers. The squeezing pressure was 3.5 bar N_2. By pressing, the pore water was filtered over 0.22 μm cellulose acetate filters, collected in acid-washed snap caps (50 ml) and stored at 4°C after acidifying with 6N suprapure HCl to a pH of 1.5 to 2.0. The squeezed sediment samples were then freeze-dried.

Oxygen in the sediment was measured by Drs. Joop Bakker and Dr. Wim Helder using both micro and needle electrodes. The details of these measurements are given in Helder & Bakker, (1985). The concentrations of nitrate, Fe and Mn in pore water were estimated spectrophotometrically (Grasshoff *et al.*, 1983).

Selective sequential extraction:

The determination of the amount of chemical phase in which each element can be present cannot be done satisfactorily, because of the fact that many phases are not crystalline, but instead are amorphous or adsorbed. An ideal extractant should remove one or a few phases of interest while resulting in negligible dissolution of other sedimentary components. In reality, such ideal behaviour of an extractant is rare, though one can find a large number of extractants and extraction methods in the literature. Recently, Robbins *et al.* (1984) have reported the development of a fairly satisfactory sequential extraction procedure for partitioning marine sediments into operationally defined fractions, after an extensive testing of each of the extraction procedures upon a range of typical marine sediments and typical sedimentary minerals.

In the present study, the selective sequential extraction procedure used was essentially from ROBBINS *et al.* (1984). Freeze-dried and homogenized sediment samples (0.5 g) were treated with different extractants and each extraction procedure involved vortex mixing, ultrasonic dispersion, centrifugation, supernate removal and combination of aliquots from repetitive treatments. The extraction sequence was modified by RUTGERS VAN DER LOEFF & WAIJERS (1986) by including an extractant suggested by CHESTER & HUGHES (1967) and also a 1.0n.HCl leach at the end. The details of the sequential extractions are given in Table I.

To estimate the total content of the metals, an acid digestion using concentrated HF and aqua regia in Teflon bombs was carried out with bulk sediment samples (RANTALA & LORING, 1975).

Each of the leaches from sequential extraction treatment and acid digested samples for total fraction was analysed by flame AAS for Mn, Fe and Zn and by graphite furnace atomic absorption spectrophotometry for Cu, Co, Ni and As.

3. Results and discussion

Distribution of extractable Fe and Mn in relation to O_2 penetration and Fe and Mn in pore water

During the mineralization of organic matter, oxygen is consumed and as a result the dissolved oxygen concentration decreases with increasing depth in the sediment. In the cores from the Skagerrak, the oxygen penetration was found to be very shallow: 2 mm in core 3, 3 mm in core 4, and 15 mm in core 11 (Fig. 3.). Very thin oxygen penetration in the Skagerrak is due to the large input of terrigenous organic matter associated with high sedimentation rate. RUTGERS VAN DER LOEFF & WAIJERS (1986) found an oxygen penetration depth between 50 and 100 cm in the Atlantic and at some locations on hillside slopes it was more than 2 m. The present observation of three cores indicates a usual trend of increasing oxygen penetration depth with increasing water depth that results from a decreasing supply of organic matter.

Dissolved manganese and iron in porewater began to increase from the top layer of core 4, in which oxygen was found to be depleted completely at 3 mm depth (Fig. 4A). Porewater NO_3 shows a depleting trend from the top layer and at 1.0-1.5 cm depth a small increase; NO_3 is uniformly low in the downcore. The porewater profiles of NO_3, Mn, Fe suggest that the top 1 or 2 cm layer might have been lost during coring or might have been eroded due to the bottom currents at this slope location of the core. Porewater Mn reaching a maximum gradient of 60 μmol.l^{-1} at a depth of 2.5 cm displays an almost linear gradient below this depth (Fig. 4A). Porewater Fe showing a maximum of 62 μmol.l^{-1} at 3.5 cm is uniform in the downcore. In core 11, oxygen reduction at 10 mm depth is followed by NO_3 reduction and then by an increase in porewater Mn (Fig. 4B) reaching a maximum of 46.5 μmol.l^{-1} at a depth of 9 cm. Porewater iron is uniformly low (between 1.5-3 μmol.l^{-1}) to a depth of 35 mm, then begins to increase in the downcore. Mn increase occurs at a depth of 15 mm.

The Mn oxyhydroxide fraction (HAM leach) in solids in core 11 shows a high value (up to 320 μmol/kg) at a depth of 2.5 to 12.5 mm. The vertical profiles of porewater Mn and of the Mn oxyhydroxide fraction in solid indicate an oxidized Mn zone in the top 7.5 to 12.5 mm (Fig. 5C) and below this a reduced Mn zone. In the reduced Mn zone dissolved Mn mostly occurs as Mn (II). The distribution of solid Mn oxyhydroxide in core 3 also shows a largely similar distribution pattern, though it presents a small variation, *viz.* the Mn oxyhydroxide fraction from the top layer decreasing to a depth of 7.5 mm and then increasing in downcore to a maximum at 20 mm (Fig. 5A). Core 4 presents an entirely different vertical profile of solid extractable fractions. More than 95% of the extractable Mn was found to be present in the HAC fraction (pH 5.0 acetic acid leach) showing that most of the extractable Mn in this core is present either in sorbed form or in the carbonate lattice structures (Fig. 5B).

Another striking difference between cores 4 and 11 is that solid phase Mn (both extractable and total) is 10 times higher in core 11 than the other 2 cores, whereas the dissolved Mn concentration in porewater in core 4 was at least two times as high as in core 11.

Sedimentation flux and accumulation rate of various metals in the Skagerrak

Table II gives the sediment accumulation rate and sedimentation flux rate in the 3 cores studied for the different metals.

$Ae = Ce\ S.\varrho t\ (1\text{-}Xw)$ where Ae is the accumulation rate of an element, Ce the concentration of the element (% weight), S the sedimentation rate ($cm.10^{-3}.yr^{-1}$), ϱt wet bulk density and Xw the weight fraction of water. The sedimentation flux rate was calculated by a simple formula given by MARCHIG & REYES (1984). In calculating the sedimentation flux rate (ϕ), the concentration gradient of the element (Δe) used was between the Mn oxic zone and Mn reduced zone, and thus the values for ϕ indicate the flux of the element between the zone of precipitation and zone of dissolution, although in the present study a steady state flux is assumed. Table II shows that the flux rate for Mn represented 50-84% of the accumulation rate for cores 3 and 4 and 89% in core 11. This suggests that the cycling of manganese between the oxidizing and reducing zone of the sediment, as it was found (SUNDBY & SILVERBERG, 1985) in the Laurentian Trough, might be quantitatively more important in the Skagerrak. Whereas core 11 shows the highest rates of Ae and ϕ for Mn, core 4 shows higher rates of accumulation and flux as far as other metals are concerned. This is due to the higher sedimentation rate at station 4 (2.4 mm/y) than at station 11 (1.6 mm/y). Studies on trends of modern rates of sediment accumulation in the Skagerrak in the last 150 years show that average sedimentation rates were varying between 1.6 and 11 mm/year with a high rate of sedimentation in the NE slope. These results seem to reflect export of fine-grained particles from higher energetic shallow-water environments in the North Sea and Baltic (ERLENKEUSER, 1985).

Table IV gives a comparison of the 3 cores in the enrichment (surface/background) factor for Mn in HAM leach and total Mn. Core 11 shows a very high enrichment factor (221) for Mn in HAM leach, 7 times higher than core 3 and 11 times higher than core 4. The enrichment factor for total Mn in core 11 was only 1.5 to 4 times higher than in the other cores. These results suggest that the higher enrichment in core 11 could only be due to the faster diagenetic remobilization of Mn in core 11, where the sedimentation rate was found to be lower (only 1.6 mm/y). ELDERFIELD & HEPWORTH (1975) found that diagenetic remobilization contributes significantly to the processes that cause metal deposition on the sediment surfaces. They concluded from their results in the Conway estuary (Wales, U.K.) that observations of metal enrichment of about 10% at the sediment-water interface, compared with the background values of the sediment, need not necessarily be interpreted as evidence of recent anthropogenic input and may instead be a consequence of sediment diagenesis.

Mn in the HAC leach in core 3 is uniform in top layers up to 35 mm and decreases below. Core 4 shows a peak at 25 mm and core 11 similarly shows a peak at 35 mm (Fig. 5). LYLE *et al.* (1984) suggested that the sorbed concentration of Mn (HAC leach) seemed to be influenced by the Mn(IV)-Mn(II) redox boundary. But the present study indicates that the sorbed concentration of Mn (HAC leach) is likely to be influenced by Fe(III)-Fe(II) redox boundary. The Mn oxyhydroxide fraction (HAM leach) of Mn is reflecting more the Mn redox boundary (Table III). Likewise, in one core (core 11) the Fe concentration in HAC leach increases with the increase in porewater Fe at 50 mm (Fe(III)-Fe(II) boundary layer).

Distribution of trace metals over the various phases

Manganese: Most of the Mn (82-99%) in these sediments was extractable (*i.e.* removed by the successive extractants up to and including the dilute acid leach), but in core 4, below 50 mm, only 65% was extractable (Fig. 9). More than 80% of extractable Mn was leached by HAM in cores 3 and 11, but instead, in core 4, 50-80% of extractable Mn was leached by HAC. Mn in HAM leach was not showing a uniform distribution in all three cores (Fig. 5), each behaving differently from the other. But uniformly, the top layers of all 3 cores showed higher levels of HAM fraction of Mn, and below 20 mm the extractable Mn diminished drastically.

Iron: Total extractable Fe was 19-25% in core 3, 9-13% in core 4 and 30-40% in core 11 (Figs 10-12). Extractable Fe did not reduce drastically in downcore as was the case with Mn. HAM and CH leaches were almost equal in all cores. Fe concentration in HAC leach was gradually increasing in deeper layers, whereas the other three phases were decreasing. At the Fe(III)-Fe(II) redox boundary, CH and HCl fractions showed an increase before they began to decrease in deeper layers.

Zinc: 20-40% of total Zn was extractable by the successive extractants; CH leach showed 74% extractable Zn at a depth of 5-10 mm in core 3 (Fig. 6). In core 4, HAC leach showed a peak at 25 mm depth (34%), CH leach seems to be significant as far as Zn is concerned. In core 11, HCl leach showed no zinc. The results indicate that zinc may be remobilized along with Fe-oxyhydroxide and sulphides. There was no difference in extractable Zn among the 3 cores, though the total Zn content was twice higher in cores 4 and 11.

Cobalt: 25-50% of the total cobalt in all cores came as totally extractable in all 4 phases. It was minimum in core 4 (25-32%) and maximum in core 11 (30-52%). HAC leach in core 4 was considerably higher than in cores 3 and 11, where it was uniformly less (Fig. 7). HAM leach was dominant in cores 11 and 3, whereas core 4 showed higher HCl leach. Though extractable fractions vary considerably from core to core, total Co was relatively uniform (Figs 10-12).

Copper: The total copper content of the sediment varied much more from core to core than did the extractable Cu (Figs 10-12). Generally, 15-30% of total Cu was extractable in all 4 phases cumulatively, except in one sample, a 20-30 mm depth sample of core 4, which showed 65.6% extractable (Fig. 7). This increase in the sample was exceptional due to the increase in content in all 4 phases (Fig. 11). In cores 3 and 11, HAM fraction was very low, whereas CH phase was showing considerable concentration. In all 3 cores, HCl fraction was the highest at almost all depths.

Nickel: Both total Ni and total extractable Ni was increasing from core 3 to core 4 to core 11. There was little variation in percentage of the total extractable Ni in all 3 cores and it varied between 13% and 23% (Figs 10-12). HAM phase was showing a peak at the Mn redox boundary layer and HCl fraction was considerable in all 3 cores (Fig. 8).

Arsenic: Of the 3 cores, core 4 had the highest total As content (73 to 192 μg/g) but the total extractable was higher in core 11 (14-59 μg/g). Generally, the total extractable As was decreasing from top layer to the deeper layer, except for some increase in the Mn redox boundary layer (Figs 10-12). In core 3 the extractable As decreased from 32% (surface) to 0.05% at 100 mm; in core 4 from 24% to 6% and in core 11 from 33% to 14%. Below 40-50 mm depth As was mostly present in not easily extractable form or it was incorporated in some form in the lattice structures. CH phase was either very low or nil in all 3 cores (Fig. 8). HCl fraction seems to be the maximum and HAM phase shows higher values at the top layer, indicating the possible exchange of As from the sediment to the overlying water.

Distribution of $CaCO_3$ and its relation to Mn distribution:

Core 4 shows a unique distribution pattern of extractable and total Mn. 90-99% of total extractable Mn from the sediments of all depths was found to be in the carbonate phase. Mn in the CO_3 phase (hitherto regarded as Mn (HAC) because of its extractant being acetic acid + acetate) also showed a spike at 25 mm depth in core 4 (Fig. 6). The $CaCO_3$ content decreased from the surface (11-12%) to 35 mm depth (9%). Mn/Ca ratio in these samples at the surface sediments was 20.97 mMol/Mole of Ca, decreased to 10.49 at 12.5 mm and started increasing below this depth. At 25 mm it was 30.97 mMole/Mole of Ca and below this it began to decrease again.

Fig. 13 shows the distribution of $CaCO_3$ (%), total Mn and Mn in HAC phase in the sediment samples of the 3 cores. There is a general decreasing trend in the concentration of Mn, while there is an increase in $CaCO_3$ content, not only in the reducing zone but also in the oxic zone of the sediment. This inverse relationship is seen most clearly in core 4.

It could be presumed that Mn is concentrated on the sediment surfaces as $MnCO_3$ but it is not very clear whether this surface Mn exists as adsorbed ions or as a surface coating. McBride (1979) showed through laboratory experiments that calcium carbonate can adsorb manganese in $MnCO_3$-undersaturated solutions and that a manganese carbonate phase was formed when saturation was reached. Franklin & Morse (1982) reported experimental results on the adsorption of manganous ions from seawater solutions. Further, Martin & Knauer (1982) found that 'weakly leachable' manganese in particle traps was associated with the calcium carbonate phase. Suess (1979) showed that microbial decomposition of organic matter in recent sediments of the Central Baltic Sea resulted in the formation of a characteristic assemblage of authigenic mineral precipitates of carbonates, sulphides, phosphates and amorphous silica. The dominant crystalline phases were found to be a mixed Mn-carbonate $[(Mn_{0.85}Ca_{0.10}Mg)CO_3]$ Mn-sulphide (MnS) and Fe-carbonate ($FeCO_3$) and Mn-phosphate $[Mn_3(PO_4)_2]$. The bulk chemical composition of acid-leachable portions of sediment cores from the Baltic showed that carbonate, containing dominantly Mn, was the most abundant phase (Suess, 1979).

Ni/Cu ratio in HAC leach

Various studies indicate that secondary dissolution, sorption and precipitation reactions actually control the dissolved constituents and oxidants instead of decomposition reactions based solely on microbial sulphate, nitrate and carbonate reduction models (SUESS, 1976, BENDER *et al.*, 1977, MURRAY *et al.*, 1978, SHOLKOVITZ, 1973). In environments of rapid sediment accumulation and those with higher rates of input of organic matter (*e.g.* the Skagerrak) interstitial metabolite concentrations exceed solubilities of certain inorganic equilibria resulting in the formation of authigenic minerals (BERNER, 1972, BRICKER & TROUP, 1975). The profile of the Ni/Cu ratio in HAC leach (Fig. 14) also shows some interesting results. The Ni/Cu ratio in cores 3 and 4 falls to a low level at 35.0 mm and 25.0 mm, respectively, these depths being the Fe(III)-Fe(II) redox boundary depths. This is mainly due to the dramatic increase in Cu concentration in HAC leach at these depths. But in core 11, the Ni/Cu ratio shows two minima, one at 12.5 mm and another at 35.0 mm. Since Ni concentration in HAC leach in all three cores does not show any marked variation, the profile of the Ni/Cu ratio reflects that increased Cu in the HAC leach at the Fe redox boundary is attributed to the dissolution of Fe oxyhydroxide fraction during reduction, resulting in the release of Cu, followed by sorption onto the sediment particles. The low Ni/Cu ratio in all 3 cores thus coincides with Fe redox boundary layer, and so it may be due to the preferential Cu remobilization and coprecipitation with iron oxides. Ni in the HAC leach does not show any remobilization in Skagerrak cores, as was observed in MANOP core M (LYLE *et al.*, 1984).

4. Summary

The distribution of trace metals over various phases in the sediment was investigated in three cores from the Skagerrak. A sequential extraction procedure was used that distinguishes a carbonate fraction, a Mn-oxyhydroxide fraction, a Fe-hydroxide fraction, a dilute acid leachable fraction and a residual fraction. The results are discussed in relation to the redox behaviour of Fe and Mn, as derived from data of dissolved O_2, Fe and Mn in the pore water.

5. Acknowledgements

I thank Bjørn Sundby for suggesting the problem to me and for his constant guidance and encouragement. Discussions with Michiel Rutgers van der Loeff throughout the programme improved the study very much. The analytical assistance from D. Waijers is acknowledged. I thank Wim Helder and Joop Bakker for providing me with the samples. Joop Bakker also generously put his oxygen data at my disposal. Thanks to all the colleagues in NIOZ who assisted my study in one way or another, particularly to Joke Hart, Sjerry van der Gaast, Albert Kok and R.F. Nolting.

Financial assistance through UNESCO/The Netherlands 1984 Fellowship Programme made my stay in Texel possible. I thank the Director of NIO, Goa, and the Director General of CSIR, India, for granting me the study leave.

6. References

ALLER, R.C., 1980. Diagenetic processes near the sediment-water interface of Long Island Sound. II. Fe en Mn. Adv.—Geophys. **22:** 351-415.

BENDER, M.L., T.L. KU & W.S. BROECKER, 1970. Accumulation ratios of Manganese in pelagic sediments and nodules.—Earth Planet. Sci. Lett. **8:** 143-148.

BENDER, M.L., K.A. FANNING, P.N. FROELICH, G.R. HEATH & V. MAYNARD, 1977. Interstitial nitrate profiles and oxidation of sedimentary organic matter in the eastern equatorial Atlantic.—Science **198:** 605-609.

BERNER, R.A., 1972. Sulphate reduction, pyrite formation and the oceanic sulphur budget. In: D. DYRSSEN & D. JAGNER. The changing chemistry of the oceans: 347-361.

——1977. Stoichiometric models for nutrient regeneration in anoxic sediments.—Limnol. Oceanogr. **22:** 781-786.

BRICKER, O.P. & B.N. TROUP, 1975. Sediment-water exchange in Chesapeake Bay. In: L.E. CRONIN. Estuarine Research. **I:** 3-27.

CALVERT, S.E. & N.B. PRICE, 1970. Composition of manganese nodules and manganese carbonates from Loch Fyre, Scotland.—Contrib. Mineral. Petrol. **29:** 215-233.

CHESTER, R. & M.J. HUGHES, 1967. A chemical technique for the separation of ferromanganese minerals, carbonate minerals and adsorbed trace elements from pelagic sediments.—Chem. Geol. **3:** 199-212.

EISMA, D., 1981. Supply and deposition of suspended matter in the North Sea.—Spec. Publ. Int. Ass. Sed. **5:** 415-428.

EISMA, D., I. SKEI, S. WESTERLUND, J. KALF, B. MAGNUSSON, K. NAES & K. SØRENSEN, 1984. Distribution and composition of suspended particulate matter and trace metals in the Skagerrak. ICES meeting, Rostock, Feb 1984: 1-13.

ELDERFIELD, H. & A. HEPWORTH, 1975. Diagenesis, metals and pollution in estuaries.—Mar. Poll. Bull. **6:** 85-87.

ERLENKEUSER, H., 1985. Distribution of ^{210}Pb with depth in core QIK 15530-4 from the Skagerrak.—Norsk Geol. Tidsskr. **65:** 27-34.

FRANKLIN, M.L. & J.W. MORSE, 1982. The interaction of Manganese II with the surfaces of calcite in dilute solutions and seawater.—Mar. Chem.

GRASSHOFF, K., M. EHRHARDT & K. KREMLING, 1983. Methods of seawater analysis. Verlag Chemie: 1-419.

HELDER, W. & J.F. BAKKER, 1985. Shipboard comparison of micro- and mini-electrodes for measuring oxygen distribution in marine sediments.—Limnol. Oceanogr. **30:** 1106-1109.

LI, Y.H. & S. GREGORY, 1974. Diffusion of ions in seawater and in deep-sea sediments.—Geochim. Coosmochim. Acta **38:** 703-714.

LYLE, M., G.R. HEATH & J.M. ROBBINS, 1984. Transport and release of transition elements during early diagenesis: sequential leaching of sediments from MANOP sites M and H. Part I. pH 5 acetic acid leach.—Geochim Cosmochim. Acta **48:** 1705-1715.

MARCHIG, V. & J.L. REYSS, 1984. Diagenetic mobilization of manganese in Peru Basin sediments.—Geochim. Cosmochim Acta **48:** 1349-1352.

MARTIN, J.H. & G.A. KNAUER, 1982. VERTEX: Manganese transport with $CaCO_3$.—Deep Sea Res.**30:** 411-425.

McBride, M.B., 1979. Chemisorption and precipitation of Mn^{2+} at $CaCO_3$ surfaces.—Soil Sci. Soc. Amer. J. **43:** 693-698.

Muller, G. & G. Irion, 1984. Chronology of heavy metal contamination in sediments from the Skagerrak (North Sea).—Mitt. Geol.-Paleont. Inst. Univ. Hamburg **56:** 413-421.

Murray, I.W., V. Grundmanis & W.M. Smeltie, 1978. Interstitial water chemistry in sediments of Saanich Inlet.—Geochim. Cosmochim Acta **42:** 1011-1026.

Price, N.B., 1976. Chemical diagenesis in sediments. In: J.P. Riley & R. Chester. Chemical Oceanography. **6** (2)**:** 1-58.

Rantala, R.R. & D.H. Loring, 1975. Multielement analysis of silicate rocks and marine sediments by atomic absorption spectophotometry.—At. Absorpt. Newslett. **14:** 117-120.

Robbins, J., G.R. Heath & M.W. Lyle, 1984. A sequential extraction procedure for partitioning elements among coexisting phases in marine sediments. Corvallis, Oregon State Univ., College Oceanogr. Rep. 84-3: 1-55.

Rutgers van der loeff, M.M. & D.A. Waijers, 1986a. The effect of oxygen tension in the sediment on the behaviour of waste radionuclides at the NEA Atlantic dumpsite. In: R.A. Bulman & J.R. Cooper (Eds.): Speciation of fission and activation products in the environment. Elsevier, Lond.

Sholkovitz, E., 1973. Interstitial water chemistry of the Santa Barbara Basin sediments.—Geochim. Cosmochim. Acta **37:** 2043-2073.

Singh, S., 1983. Geochemistry and sedimentology in holocene and recent sediments from Skagerrak. Thesis, Univ. Oslo, 1983: 1-120.

Skei, I.M., 1981. The entrapment of pollutants in Norwegian fjord sediments - a beneficial situation for the North Sea.—Spec. Publ. Int. Ass. Sediment **5:** 461-465.

Suess, E., 1976. Nutrients near the depositional interface. In: N. McCave. The Benthic Boundary Layer. New York, Plenum Press: 57-80.

Suess, E. & H. Erlenkeuser, 1975. Anthropogenic metal and carbon input in Baltic Sea sedimentary basins. In: M. Brüderlin. Geoscientific Studies and the potential of the Natural Environment. Deutsche UNESCO Kommission, Köln: 203-214.

Sundby, B. & N. Silverberg, 1985. Manganese fluxes in the benthic boundary layer.—Limnol. Oceanogr. **30:** 372-381.

Weering, T.C.E. van, 1982. Marine geological investigations in the Skagerrak, northeastern North Sea. Thesis, Groningen Univ.: 1-201.

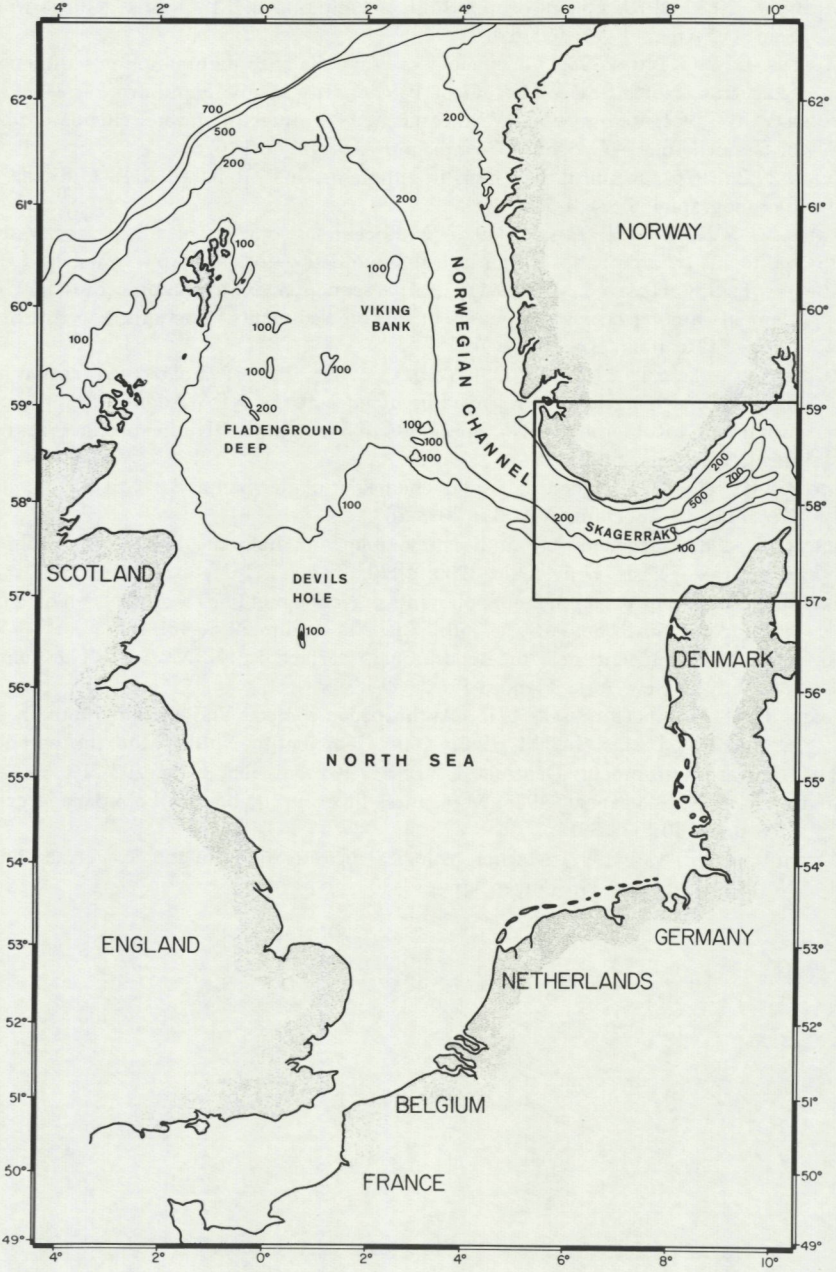

Fig. 1. Map of the Skagerrak Sea.

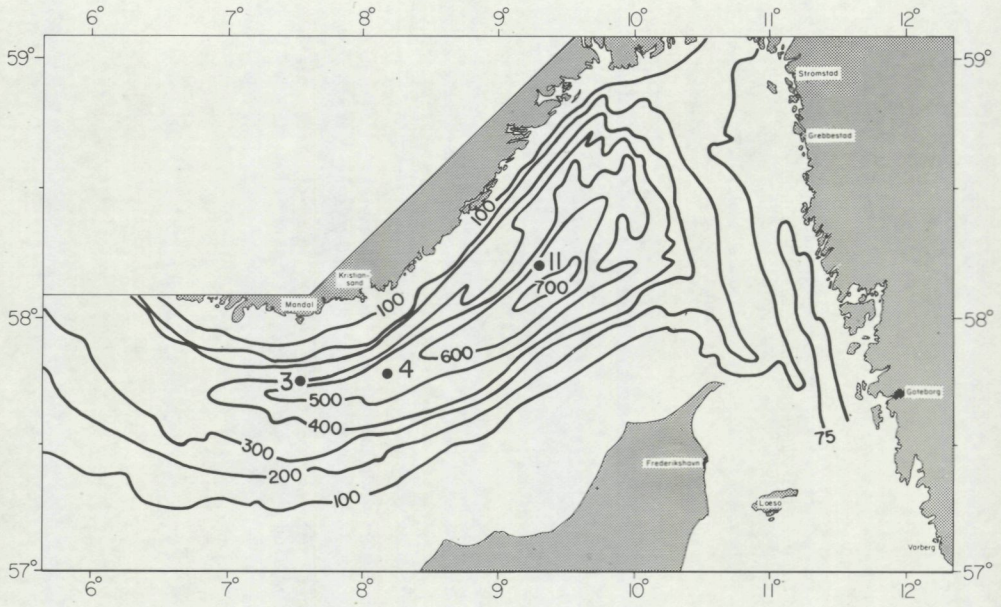

Fig. 2. Map of the Skagerrak showing sampling stations and bathymetry.

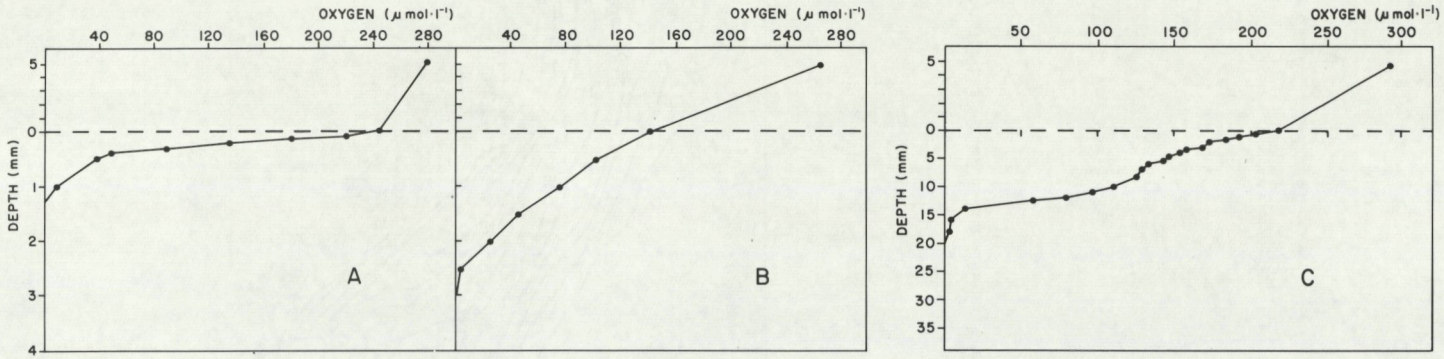

Fig. 3. Vertical profile of oxygen penetration in (A) core 3 (B) core 4 and (C) core 11. Note the change in vertical scale for core 11.

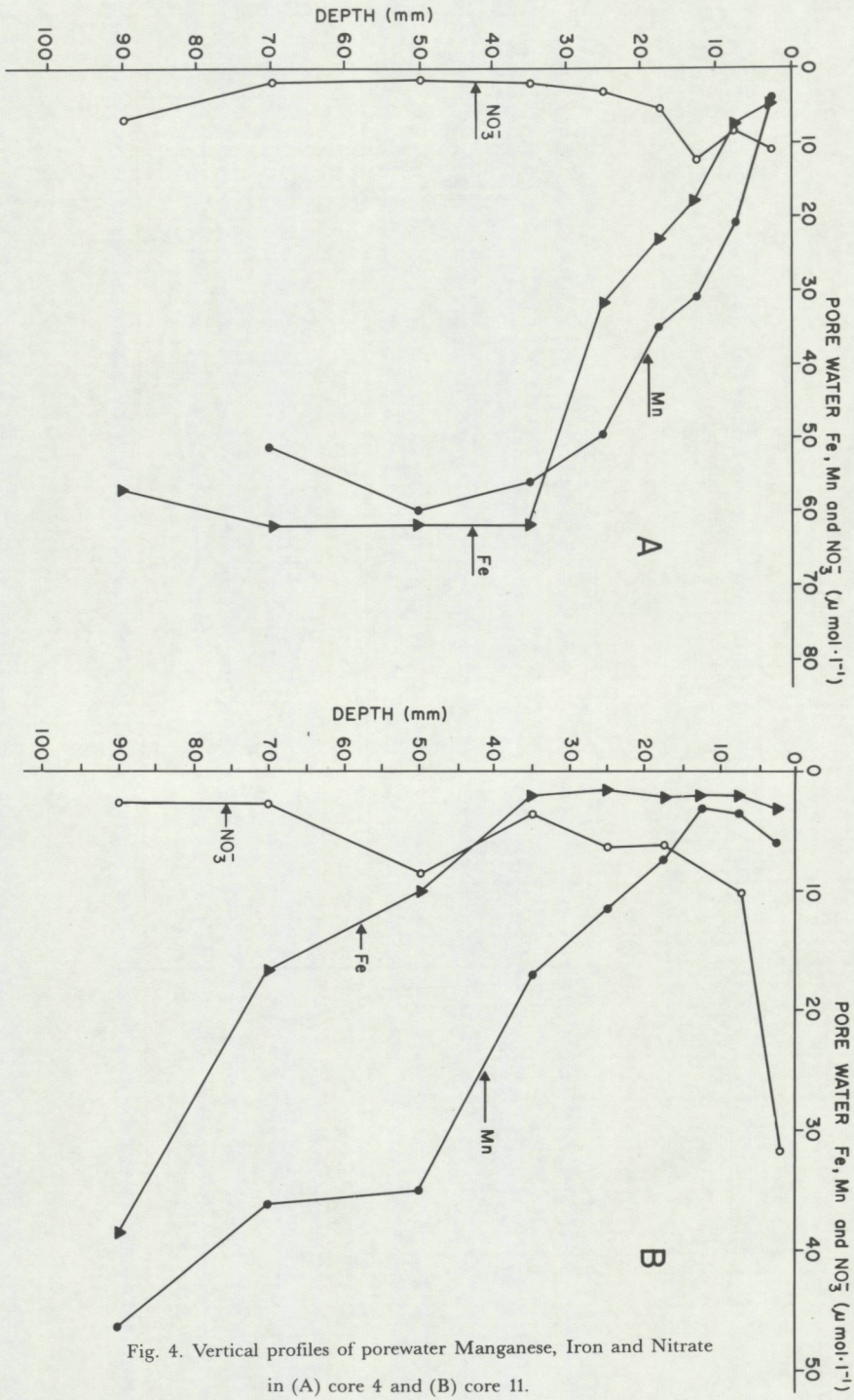

Fig. 4. Vertical profiles of porewater Manganese, Iron and Nitrate in (A) core 4 and (B) core 11.

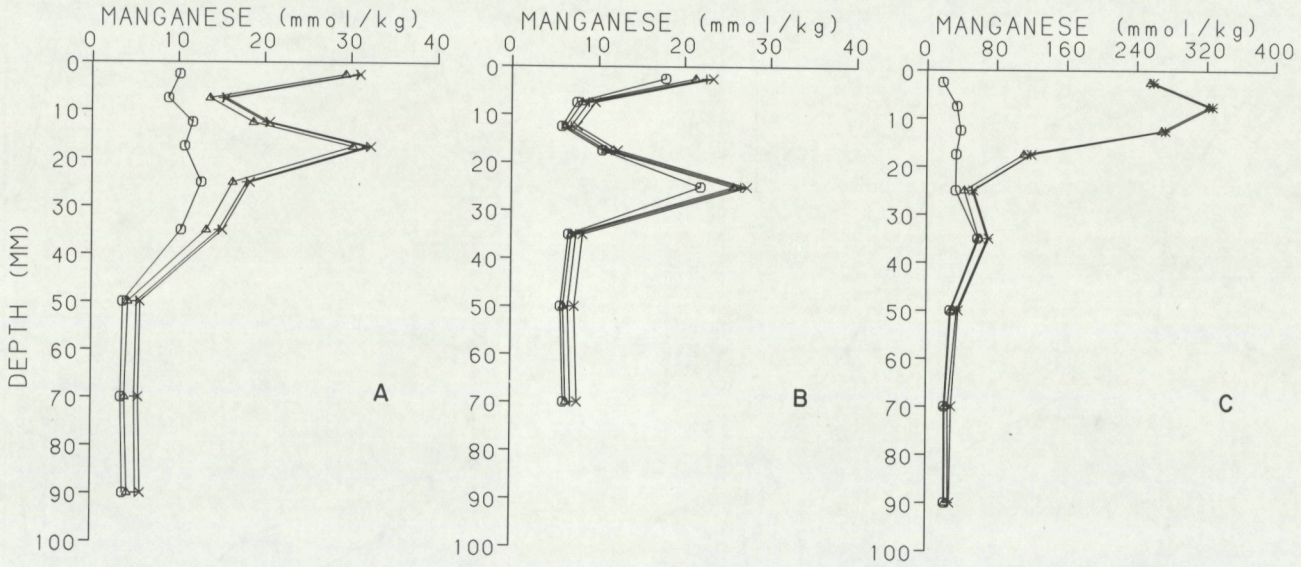

Fig. 5. Vertical profile of different extractable phases of Manganese (cumulative concentration) in (A) core 3, (B) core 4 and (C) core 11. (o) HAC, (Δ) HAM, (+) CH and (x) HCl.

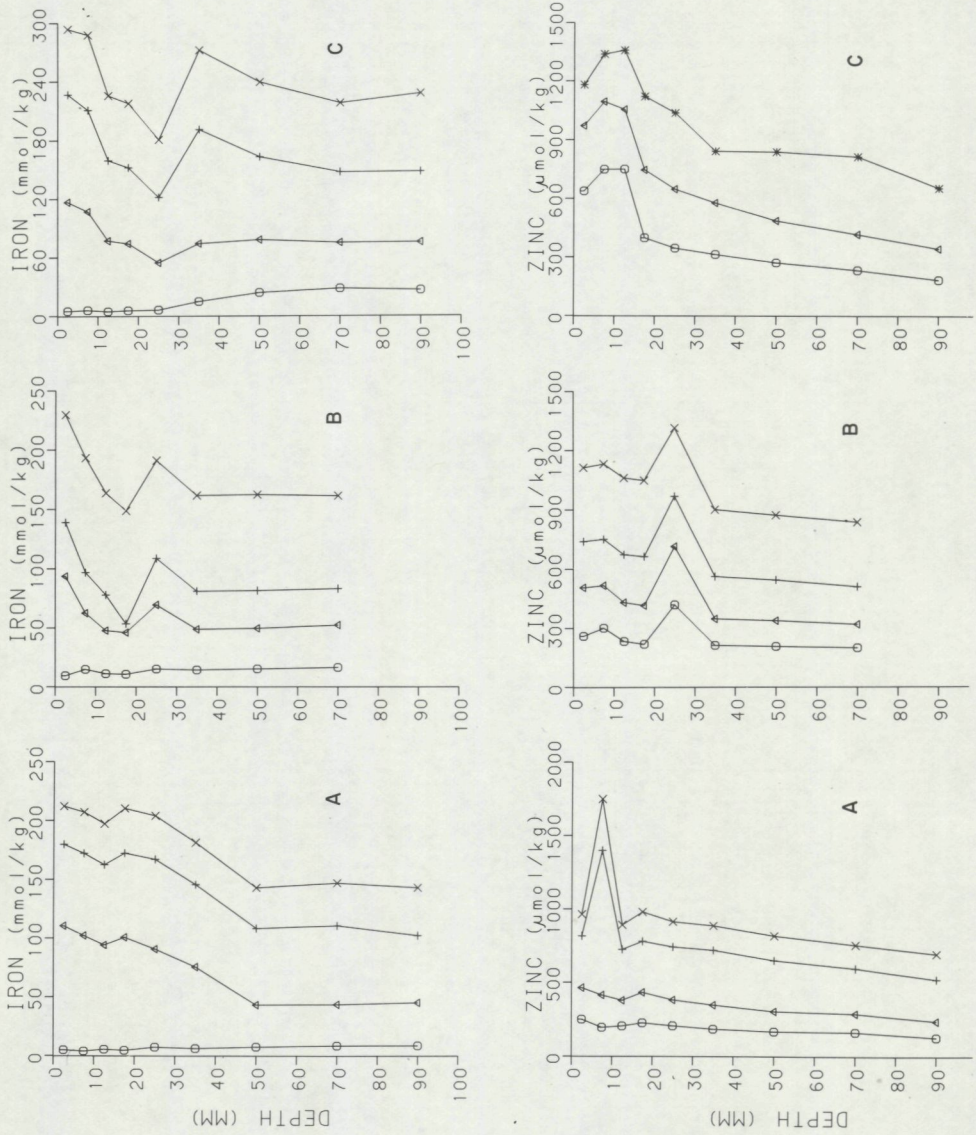

Fig. 6. Vertical profile of different extractable phases of Iron and Zinc: (A) core 3, (B) core 4 and (C) core 11. (o) HAC, (Δ) HAM , (+) CH and (x) HCl.

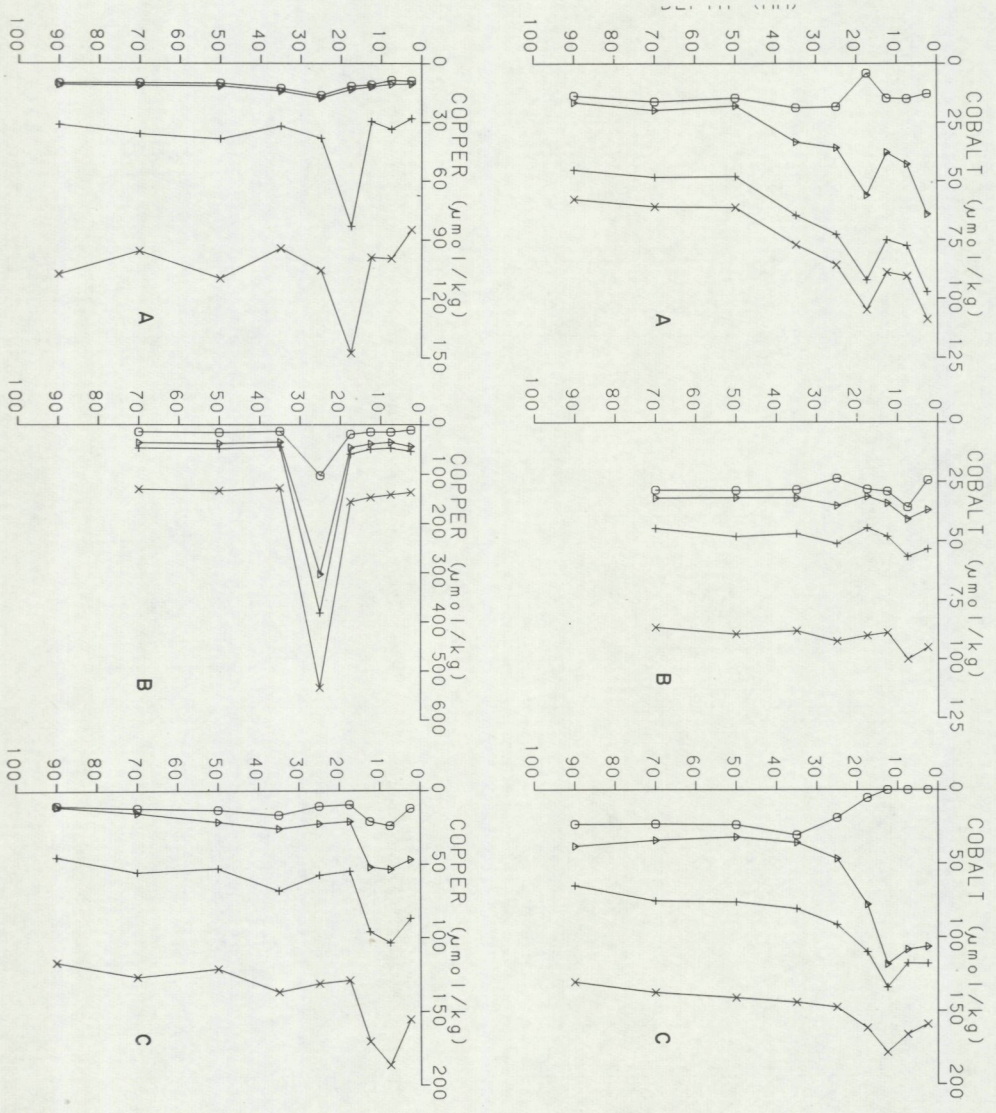

Fig. 7. Distribution of cumulative concentration of different extractable phases of Cobalt and Copper. Explanation of symbols as in Fig. 5.

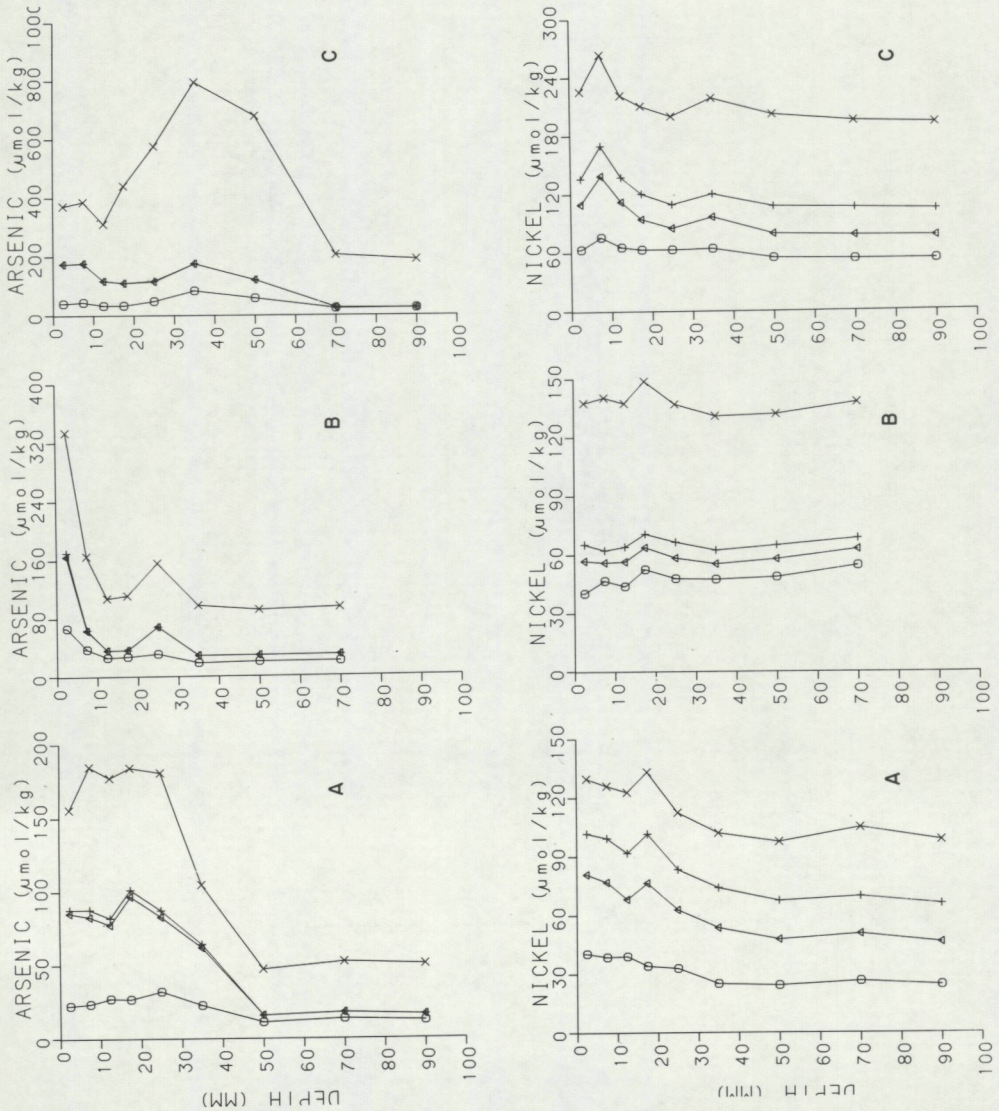

Fig. 8. Distribution of cumulative concentration of different extractable phases of Arsenic and Nickel. Explanation of symbols as in Fig. 5.

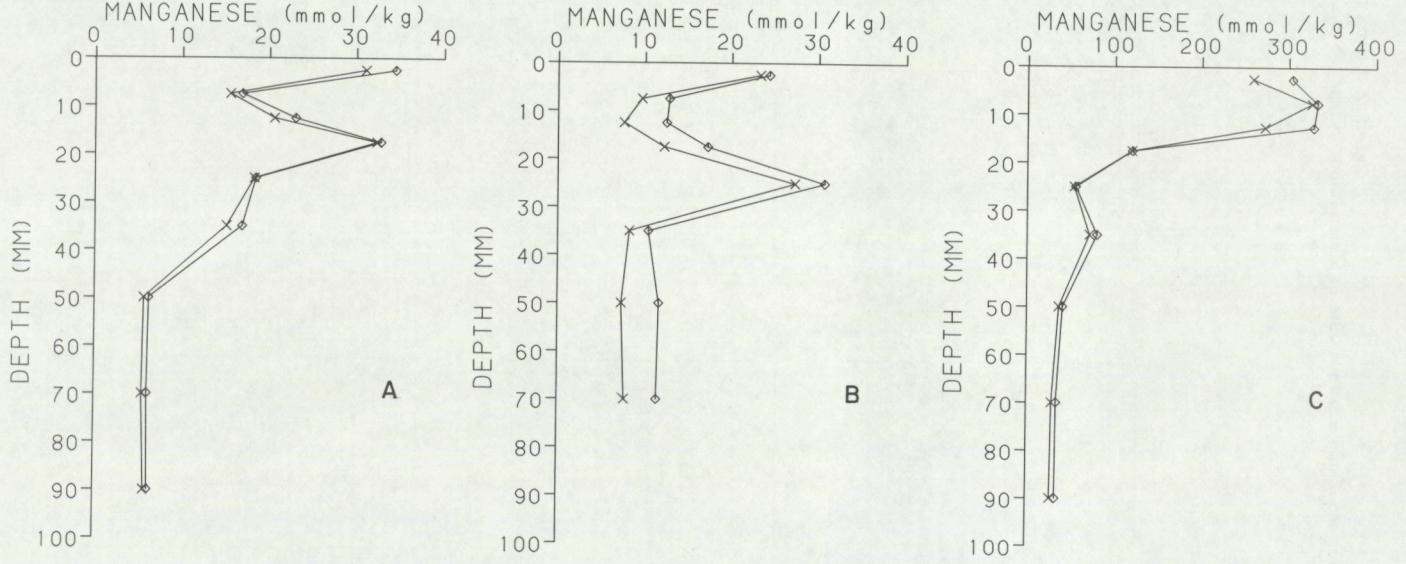

Fig. 9. Vertical profile of extractable and total Mn in (A) core 3, (B) core 4 and (C) core 11. (x) total extractable metal and (◊) total content.

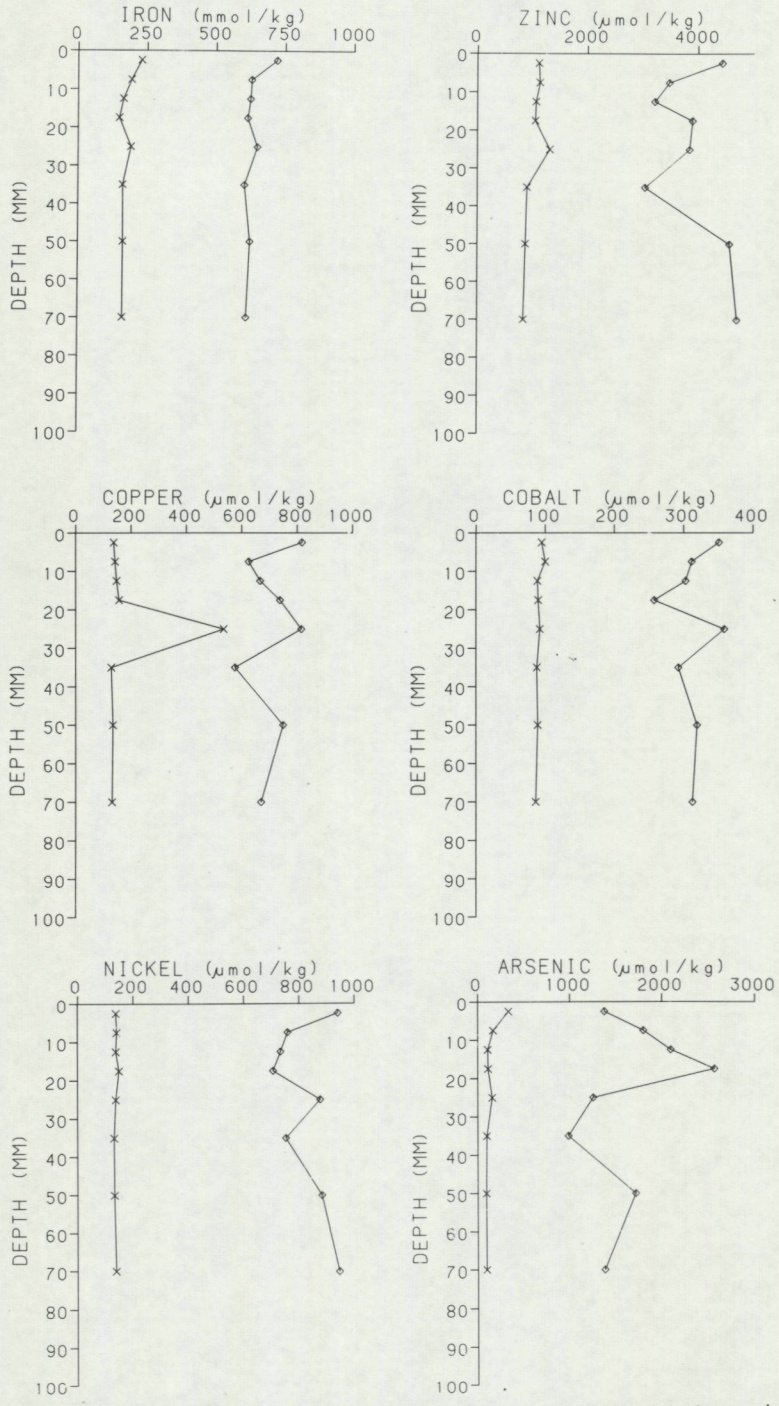

Fig. 10. Vertical profile of extractable and total metals in core 3. Explanations as in Fig. 9.

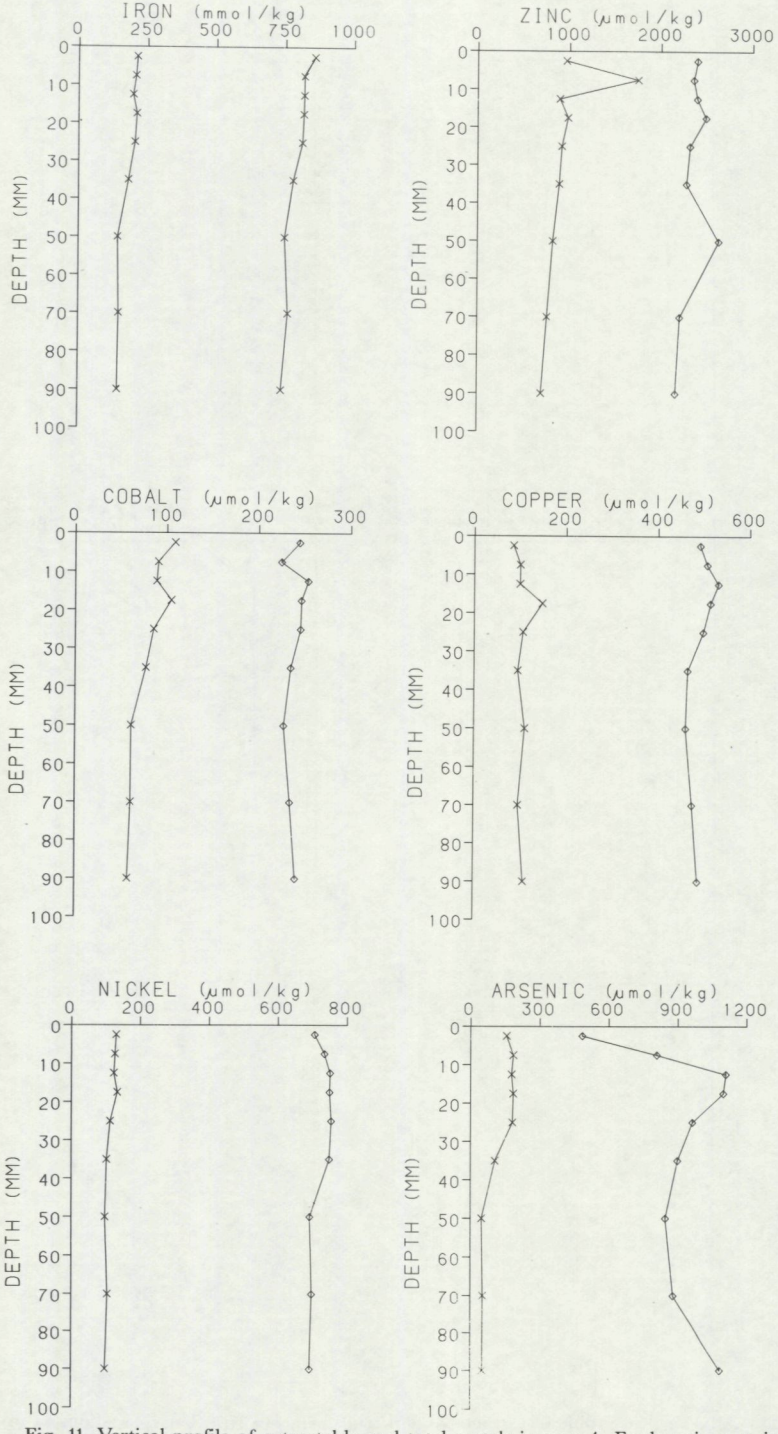

Fig. 11. Vertical profile of extractable and total metals in core 4. Explanations as in Fig. 9.

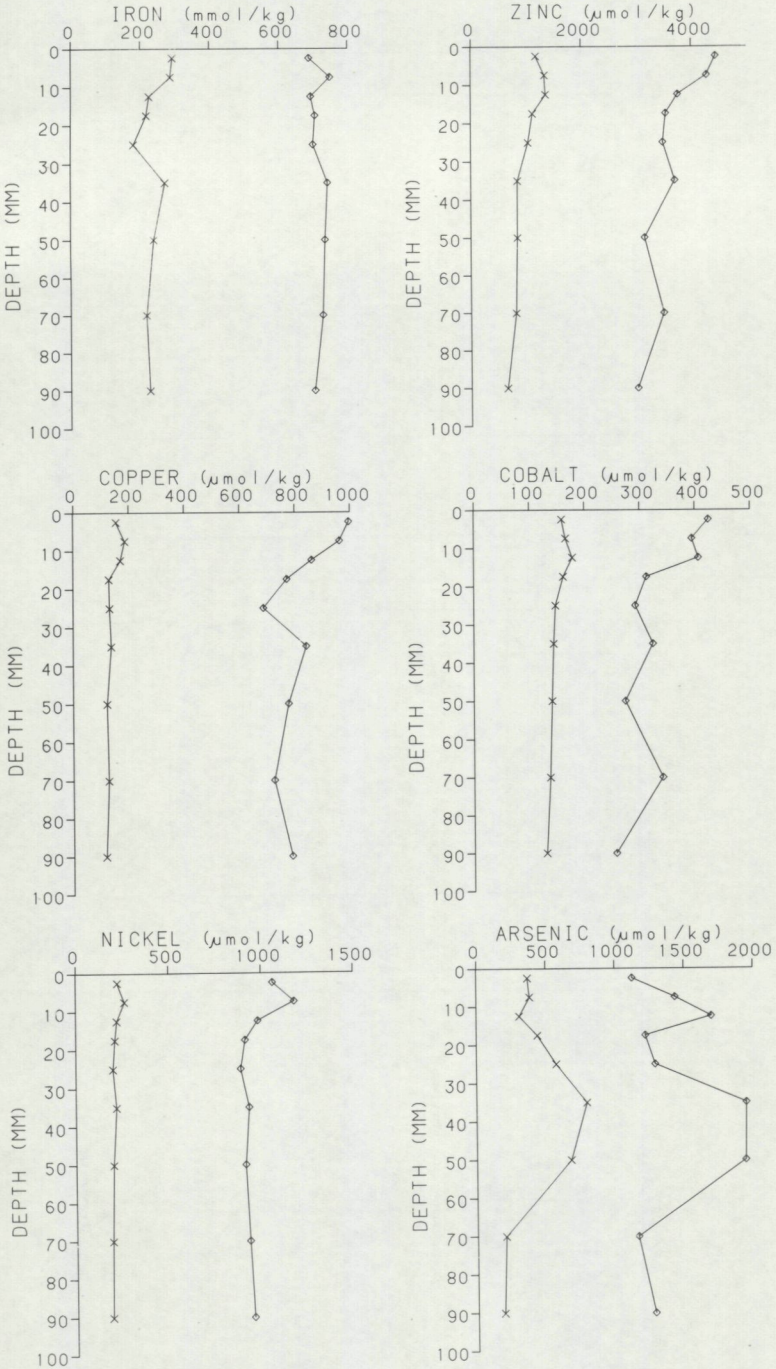

Fig. 12. Vertical profile of extractable and total metals in core 11. Explanations as in Fig. 9.

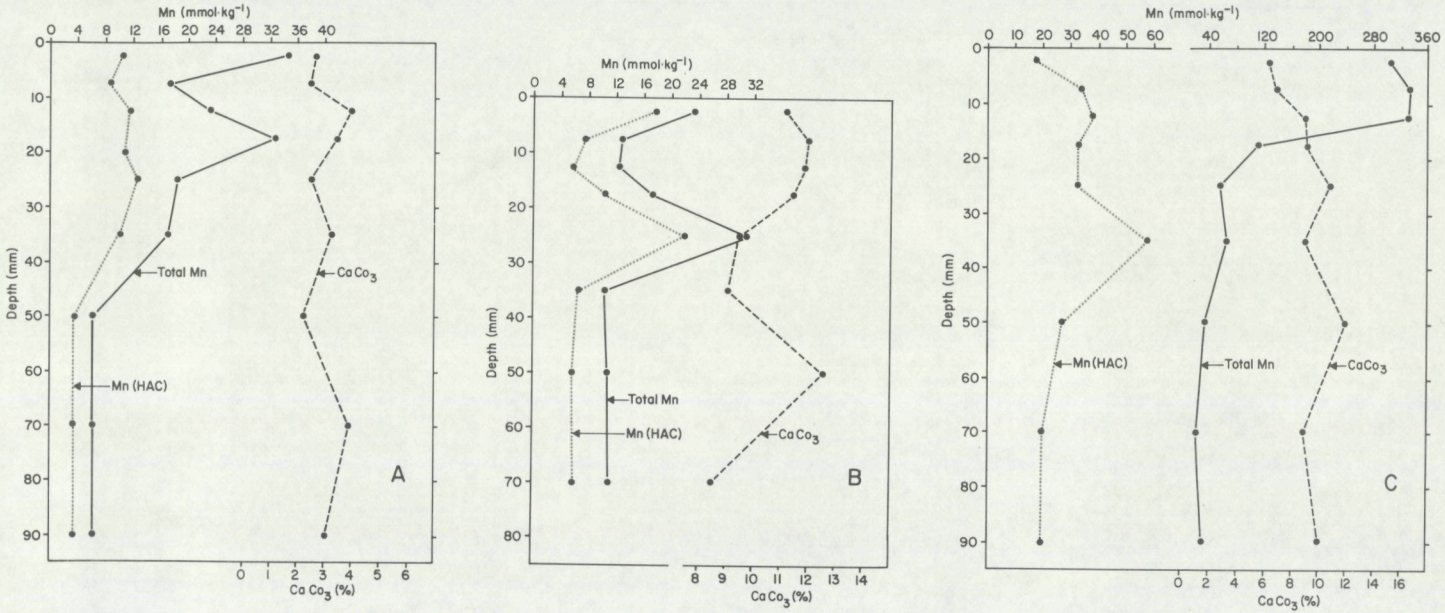

Fig. 13. Distribution of $CaCO_3$ (%), total Mn and Mn in HAC leach in (A) core 3, (B) core 4 and (C) core 11.

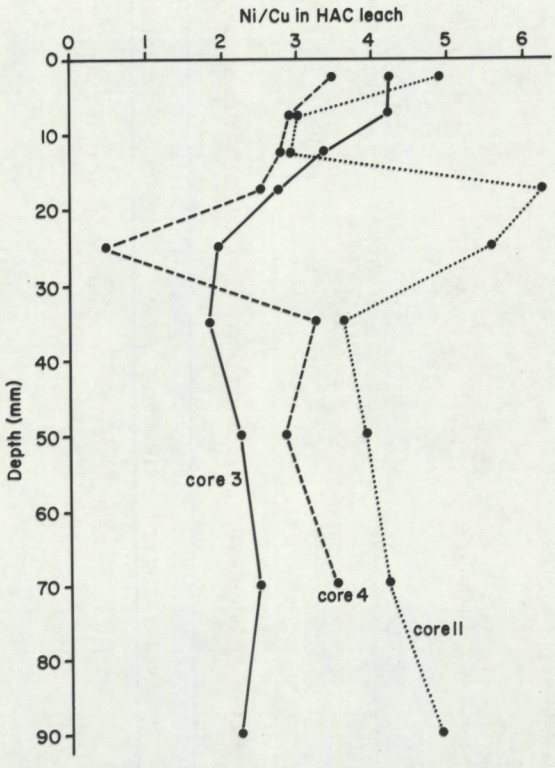

Fig. 14. Vertical profile of the Ni/Cu ratio in HAC leach.

Table I: Sequential Extraction Procedure

Name	Extractant	Repeat	Resultant fraction	Reference
1) HAC	NaOAc (1M) + HOAc, pH 5.0	3	carbonate, sorbed and salts	Robbins et al. (1984)
	NaCl (0.2 M) wash	1	discard	
2) HAM	$NH_2OH.HCl$ (1M) + Na.citrate (0.175 M), pH 5.	3	Mn-oxyhydroxide	Robbins et al. (1984)
3) CH	$NH_2OH.HCl$ (1M) + HOAc (25% v/v) pH 2.5	3	Fe-oxyhydroxide	Chester and Hughes (1967
4) HCl	HCl (1.0N)	3	residual leachable	

Table II: Accumulation rates and sedimentation flux rate of different metals

Element	Core 3		Core 4		Core 11	
	Ae	O	Ae	O	Ae	O
Manganese	31	26	27	13	227	202
Iron	782	109	878	134	522	34
Zinc	2.6	-	6.3	-	3.94	1.27
Copper	0.51	0.017	1.13	0.205	0.859	0.179
Cobalt	0.235	0.010	0.452	0.075	0.340	0.134
Nickel	0.677	-	1.20	-	0.849	0.086
Arsenic	1.23	-	2.25	-	1.15	-

Ae (Accumulation rate) = Ce.S.Pt(1-X) mg $cm^{-2} 10^{-3} yr^{-1}$

O (Sedimentatio. flux rate) = S.p. E mg $cm^{-2} 10^{-3} yr^{-1}$

Table III: Chemical characteristics of three cores in Skagerrak and probable Mn and Fe redox boundaries

Core no.	O_2 penetration Depth in mm	Pore water gradient Depth in mm			Sediment fractions				Mn IV-Mn II Redox boundary Depth in mm	Fe III-Fe I Redox bound Depth in mm
		NO_3	Mn	Fe	Mn gradient Depth in mm HAC	HAM	Fe gradient Depth in mm HAC	HAM		
Core 3	2	-	-	-	35	2.5	No	35	2.5	35.0
Core 4	3	2.5	2.5	25	25	2.5	No	25	2.5	25.0
Core 11	15	5.0	12.5	50	35	12.5	increase at 50 mm	35	12.5	50.0

Table IV: Enrichment factors for different metals

Core	Fe in HAM leach %			Total Fe %		
	Background value	Surface value	Enrichment	Background value	Surface value	Enrichment
3	0.195	0.589	3.02	4.115	4.785	1.16
4	0.19	0.470	2.44	3.367	4.022	1.19
11	0.262	0.623	2.38	3.93	4.183	1.06

Core	Mn in HAM leach. (ppm)			Total Mn (ppm)		
	Background value	Surface value	Enrichment	Background value	Surface value	Enrichment
3	30	1055	35	330	1893	6
4	17	192	11	627	1338	2
11	59	13025	221	1836	16727	9

Core	Zn in HAM leach. (ppm)			Total Zn (ppm)		
	Background value	Surface value	Enrichment	Background value	Surface value	Enrichment
3	7	14	2	141	157	1.1
4	7.8	16.1	2.1	199	290	1.5
11	10.4	21.8	2.1	197	290	1.5

Core	Co in HAM leach. (ppm) B	S	Enrichment	Total CO(ppm) B	S	Enrichment
3	0.17	3.02	17.8	13	14	1.08
4	0.18	0.74	4.1	18	21	1.17
11	0.89	6.28	7.6	15	25	1.67

Core	Cu in HAM leach. (ppm) B	S	Enrichment	Total Cu(ppm) B	S	Enrichment
3	0.05	0.10	2	29	31	1.07
4	1.4	2.13	1.52	42	51.9	1.05
11	0.04	2.22	55	46	63	1.04

Core	Ni in HAM Leach. (ppm) B	S	Enrichment	Total Ni (ppm) B	S	Enrichment
3	1.28	2.38	1.85	40	41	1.03
4	0.45	0.98	2.18	51	55	1.08
11	1.36	2.72	2.00	56	63	1.13

Core	AS in HAM leach (ppm) B	S	Enrichment	Total AS (ppm) B	S	Enrichment
3	0.3	4.7	15.7	81	36	-
4	0.68	7.36	10.8	103	103	-
11	0.2	10.1	50.5	90	84	-